Mine Water and the Environment (2019) 38:60–71
https://doi.org/10.1007/s10230-018-00576-z

TECHNICAL ARTICLE

Using Water Injection to Prevent Shaft Failure in the Jining No. 3 Coal Mine, China

Yanchun Xu[1] · Mingze Du[1,2] · Yaqi Luo[1]

Received: 12 June 2017 / Accepted: 22 December 2018 / Published online: 4 January 2019

Abstract

Water injection into aquifers is a new approach for preventing shaft failure by stabilizing water levels. A series of injection tests was performed in the Jining no. 3 coal mine. Injection flow rates decreased over time as the water injection channels were blocked. Groundwater elevations in four observation boreholes and strain variations in the alluvial strata and shaft walls were analyzed to assess the effect of water injection on shaft failure and determine a preventive injection rate. The groundwater elevations in the observation boreholes decreased and the compressive strains in the alluvial strata and shaft wall increased overall over time. Although the water injection effect has weakened in recent years, it has still effectively slowed the increase of compressive strain in the shaft wall compared with conditions before water injection. We determined that the total and average injection rates for the four boreholes need to be approximately 20 m^3/h and ≥ 5 m^3/h, respectively, to maintain groundwater elevations and stabilize strain in the shafts. Measures such as oscillating pressurized water injection or increasing the number of injection boreholes could be used to increase injection flow rates and prevent shaft failure.

Keywords Mining engineering · Formation compression · Additional stress · Aquifer replenishment

Introduction

The Huang Huai region of China is an important coal production area, and there are more than 300 vertical shafts passing through the thick, unconsolidated Quaternary deposits of the region. Over 100 disasters induced by mine shaft fractures have occurred in the Huang Huai region since 1987. After decades of research, construction quality, geo-stress, seepage deformation, and additional stress on shaft walls have explained the mechanism of shaft failure (Liu et al. 2011; Ni et al. 2007). The additional stress on the shaft wall has been accepted as the primary cause of failure by most scholars and engineers. Mining has lowered the water level of the deepest aquifer in the Quaternary alluvium, which resulted in consolidation and compression of the overlying strata. During strata subsidence, the frictional force increased outside the shaft wall. The frictional force produced a vertical downward compressive stress in the shaft wall, which was referred to as additional stress. The compressive stress of the shaft wall increased with depth and generally reached a maximum at the base of alluvium. Once the compressive stress surpassed the strength of the concrete, the shaft wall ruptured (Cui 1998; Cui and Cheng 1991; Gao et al. 2009; Liu et al. 2007; Lou and Su 1991; Meng et al. 2013; Wang 1996; Yu 2013). Based on the mechanism of shaft failure, methods to reinforce the shaft wall by installing a wall ring, casing the shaft wall, creating a stress-relief slot, grouting the surrounding strata, and injecting water to stabilize water levels were proposed. However, the first four methods were time-consuming and labor-intensive, and required re-treatment every few years.

In recent years, water injection into aquifers has been used to stabilize water levels and prevent shaft failure. Numerical simulation of water injection engineering parameters and water injection tests of a single borehole were carried out in the Jining no. 3 and Dongtan coal mines in China (Deng et al. 2014; Liu et al. 2017; Xu et al. 2014a, b), based on

Electronic supplementary material The online version of this article (https://doi.org/10.1007/s10230-018-00576-z) contains supplementary material, which is available to authorized users.

✉ Mingze Du
dumingze0910@163.com

[1] School of Resources and Safety Engineering, China University of Mining and Technology, Beijing 100083, China

[2] Mine Safety Technology Branch, China Coal Research Institute, Beijing 100013, China

theoretical and model tests (Wang et al. 2002; Zhou and Xu 2006). Outside of China, this approach has not been used to prevent shaft failure, but it has been applied for surface subsidence prevention and building rectification (Baek et al. 2008; Bell et al. 2001; Luo et al. 2010; Sato et al. 2003; Sheorey et al. 2000; Soni et al. 2007; Tomaz and Goran 2003; Unver and Yasitli 2006). More than 50 countries and regions have experienced land subsidence due to groundwater exploitation. The more serious incidents have occurred in Japan, the United States, Mexico, Italy, Thailand, and China. Several cities, such as Niigata, Japan; Far West Rand, South Africa; and Santa Clara, California, United States have taken measures such as recharging or reducing groundwater exploitation to control surface subsidence (Yan and Liu 1996).

The Jining no. 3 coal mine was the first coal mine in the world to use the water injection method to prevent shaft failure. The water injection project has been running for nearly 5 years and the combined injection test in the Z2, Z4, Z5, and Z6 boreholes stabilized strains in the shaft wall. However, over time, it was observed that the water injection flow rate decreased and the compressive strain in the shaft wall increased. Variations in groundwater elevations in the Q_L-1, Q_L-3, Q_L-4 and Z1 boreholes and strains in the alluvial strata and shaft wall were analyzed to evaluate the effects of water injection over time and determine a reasonable water injection rate.

Site Description and Alluvium Characteristics

The Jining no. 3 mine is located in southwestern Shandong Province in eastern China. The underground mine covers an area of 105 km^2 and has a designed production capacity of 5×10^6 metric tons per year with a service life of 81 years. The main, auxiliary, and ventilation shafts are located in an industrial square and penetrate through a thick loose aquifer. The shaft wall in the alluvium was made of composite reinforced concrete, and was constructed with the freezing method. In September 2004, fractures occurred in the wall of the ventilation shaft, and measurements for applying a stress-relief slot were taken to reduce the stress in the shaft wall. To ensure the safety of the main and auxiliary shafts, grouting and the creation of a relief slot were carried out in December 2005 and February 2005, respectively.

The influence of the alluvium and hydrodynamics on shaft failure was limited. The alluvium area and water injection tests was bounded by the main, auxiliary, and ventilation shafts (the inset in Fig. 1 shows the industrial square). The overall study area was 5000 m in length from north to south and 4000 m in width, covering an area of 20 km^2.

Based on 90 boreholes on 10 exploration lines near the shafts, the characteristics of the alluvium were obtained. The thickness of the Quaternary strata was greater than 150 m, with increasing thickness from east to west, but the variation was generally small. The alluvial strata above the bedrock

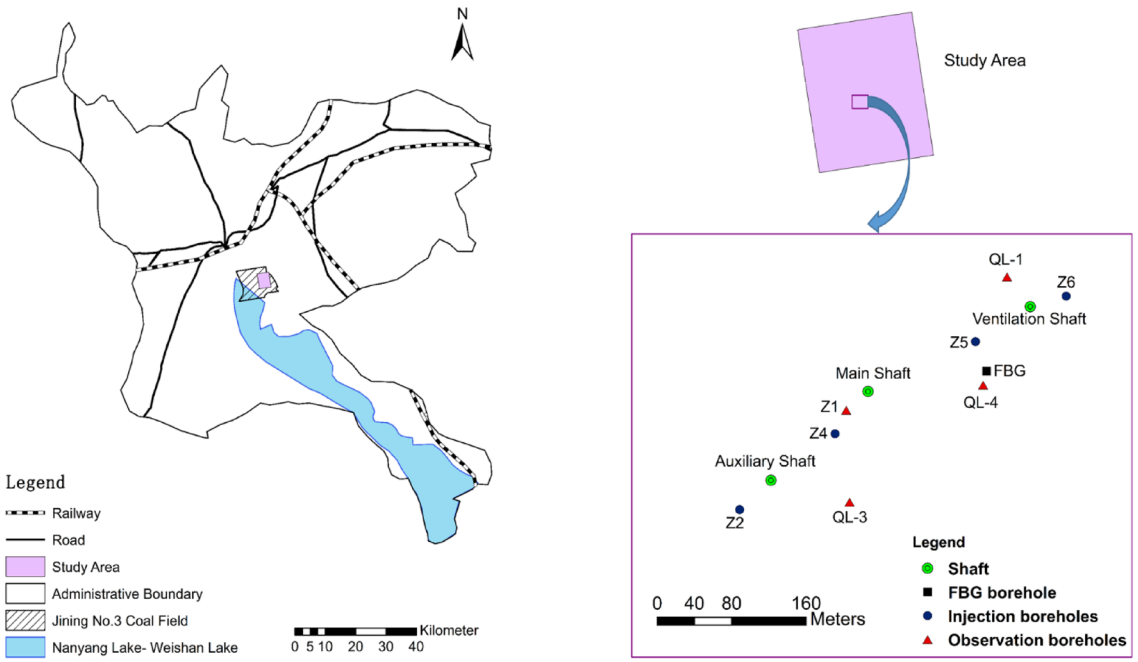

Fig. 1 Location map of the study area

are divided into three units: upper, middle, and lower. The thickness of the lowermost sand layer of alluvium near the shafts was approximately 25 m on average and gradually thickened on the north and south sides and thinned on the east and west sides. There was a clay layer, missing in some places, at the base of the alluvium, and the clay layer penetrated by the main, auxiliary, and ventilation shafts was between 4 and 10 m in thickness, which provided favorable conditions for water injection into the aquifer to stabilize the water level.

Monitoring System for the Water Injection Project

The project monitoring system had three components: water level monitoring, monitoring of strain in the alluvial strata, and monitoring of strain in the shaft wall. The injection boreholes are Z2, Z4, Z5, and Z6, and the observation boreholes for monitoring water level are Q_L-4, Q_L-1, Z1, and Q_L-3 (Table 1). Injection and monitoring depths and Fiber Bragg grating (FBG) monitoring layers for the injection tests are given in Table 1. Table 2 shows the FBG monitoring network in the FBG borehole near Q_L-4. The water level monitoring system was composed of four water level observation boreholes (Q_L-1, Q_L-3, Q_L-4, and Z1), which were located in the industrial square (see Fig. 1 inset map). The monitoring system of strain in the alluvial strata was composed of a FBG network located near the Q_L-4 borehole, with 18 sensors in 10 layers between depths of 106.2 and 176.5 m (Table 2). Because the shallowest depth of the monitored strata exceeded 100 m, the temperature in the strata was not affected by the surface temperature, and the temperature was almost constant in an individual layer. The FBG network was embedded in a glass fiber reinforced polymer encapsulated material to form the fiber grating sensor. The mechanical transmission relationship between the fiber grating and alluvial strata was: fiber grating—encapsulated material—cement mortar—alluvium, to eliminate any influence of temperature. The shaft wall monitoring system was primarily composed of strain gauges imbedded in the shaft wall. Sixteen strain gauges were installed in the ventilation shaft wall at four depths (126 m, 135 m, 147 m, and 172 m); 24 strain gauges were installed in the main shaft wall at six depths (119 m, 131 m, 143 m, 151 m, 159 m, and 167 m); and 16 strain gauges were installed in the auxiliary shaft wall at four depths (138 m, 150 m, 168 m, and 180 m).

Positive values of strain indicate tensile conditions, while negative strain values indicate compressive conditions. Tensile or compressive strain decreases as values approach zero. Strain is a dimensionless measure that is often reported as microstrain ($1\mu\varepsilon = 10^{-6}\varepsilon$).

Table 1 Injection and monitoring depths and FBG monitoring layers for the injection tests

Injection borehole ID	Injection depth (m)	Water observation borehole ID	Water level depth (m)	FBG monitoring layers (see Table 2)
Z2	142.00–171.40	Q_L-4	115.83–135.15	15, 17
Z4	141.00–165.20	Q_L-1	114.00–171.53	15, 17, 21, 22, 24, 29, 32, 34, 38
Z5	141.00–165.20	Z1	144.85–176.40	24, 29, 32, 34, 38
Z6	138.80–169.20	Q_L-3	166.00–176.00	38

Table 2 FBG monitoring network and stratigraphy in the FBG borehole near Q_L-4

FBG sensor ID	Layer #	Lithology	Thickness (m)	Cumulative depth (m)	Quaternary unit
0101, 0201	10	Sandy gravel	3.26	107.59	Upper
0206, 0301	15	Sandy gravel	3.94	121.77	Lower
0106, 0102, 0202, 0403	17	Sandy gravel	12.48	135.15	Lower
0205	21	Medium coarse sand	0.70	144.10	Lower
0302	22	Sandy gravel with clay	2.00	146.10	Lower
0105, 0203	24	Sandy gravel	3.36	149.81	Lower
0103, 0402	29	Sandy gravel	2.70	160.70	Lower
0204	32	Thin sand	1.10	163.20	Lower
0303	34	Sandy gravel with clay	1.10	164.90	Lower
0104, 0401	38	Clay	8.60	176.50	Lower

Methodology

Water Injection Process

The groundwater elevation in the deepest aquifer in the Quaternary alluvium (lower unit) was approximately 156.5–163.0 m before water injection in July 2008. Single borehole (Z1 and Q_L-4) injection tests were carried out in August 2009 and from March 2010 to April 2010 (Xu et al. 2014b). A combined injection test in the Z5 and Z6 boreholes was conducted from April 29, 2011 to June 4, 2011. Combined injection in the Z2, Z4, Z5, and Z6 boreholes officially began on July 10, 2011 and is ongoing. The start and end times of each injection stage is given in Table 3.

In consideration of mine water quality and environmental protection, treated municipal water derived from surface water in the town was used for the injections, and the water was transported from local water suppliers to the mine through pipelines. The injection pipe was sealed and connected to the drilling casing pipe and relied on pipeline pressure or a water pump to realize injection. The order of the pipeline connection was inlet pipe—water pump—valve—pressure gauge—flow meter—water injection pipe, and then to the aquifer. A photograph of the Z5 injection borehole pipe is shown in Supplemental Figure 1.

Water Injection Pressure and Flow Rate Monitoring

For the combined injection test in the Z5 and Z6 boreholes, the water injection pressure and flow rate were measured every 10 min in the first 2 h and then once every half hour on day 1. On the day 2, observations were made once per hour. Observations were made once every 8 h on days 3–8, and then once per day after day 8. In the combined injection test in the Z2, Z4, Z5 and Z6 boreholes, the water injection pressure and flow rate were monitored twice a month.

Borehole Washing

Borehole washing uses liquid carbon dioxide to create blowouts and remove the sludge inside the borehole to increase the flow rate of water injection. Borehole washing was conducted from September 5 to 10, 2014 in boreholes Z4 and Z5 and in February 2016 for borehole Z6.

Results

Because the groundwater elevation in the deepest aquifer of the Quaternary alluvium (lower unit) continued to decrease as a result of ongoing mine dewatering, the overlying strata were compressed, the stress on the shaft wall increased, and the possibility of shaft failure increased. Water injection was aimed at stabilizing water levels without producing additional stress on the shaft wall. When water injection makes groundwater elevations rise or stabilize, the strata do not experience compressive deformation, and the compressive strain in the shaft wall does not increase, indicating that water injection plays a role in preventing shaft failure.

For the combined injection test in the Z5 and Z6 boreholes and the early stage of the combined injection in the Z2, Z4, Z5 and Z6 boreholes, the groundwater elevations increased slightly, and the compressive strain in the shaft wall decreased or was relatively stable. However, over time the water injection flow rate decreased and the compressive strain in the shaft wall increased, indicating that the water injection effect weakened and the flow rate of the water injection was insufficient to decrease the stress on the shaft wall.

Borehole Washing

The depths, pressures, and flow rates for three injection boreholes before and after borehole washing are shown in Supplemental Table 1. After washing, higher flow rates were achieved.

Variation in Water Pressure and Flow Rate in the Injection Boreholes

Figure 2 shows the variations in water injection pressure and instantaneous flow rate in the injection boreholes over time. The injection pressure of the Z2 borehole was between 0.2 and 0.8 MPa, and the instantaneous flow rate was between 1 and 5 m^3/h; the injection pressure of the Z4 borehole was between 0.2 and 0.9 MPa, and the instantaneous flow rate was between

Table 3 The start and end time of each stage of water injection

Water injection stage	Water injection pressure (MPa)	Start time	End time
Single borehole injection tests	0.1, 0.3, 1	August 2009	April 2010
Combined injection test in the Z5 and Z6 boreholes	0.2–0.5	April 29, 2011	June 4, 2011
Combined injection in the Z2, Z4, Z5 and Z6 boreholes	0.04-1	July 10, 2011	Ongoing

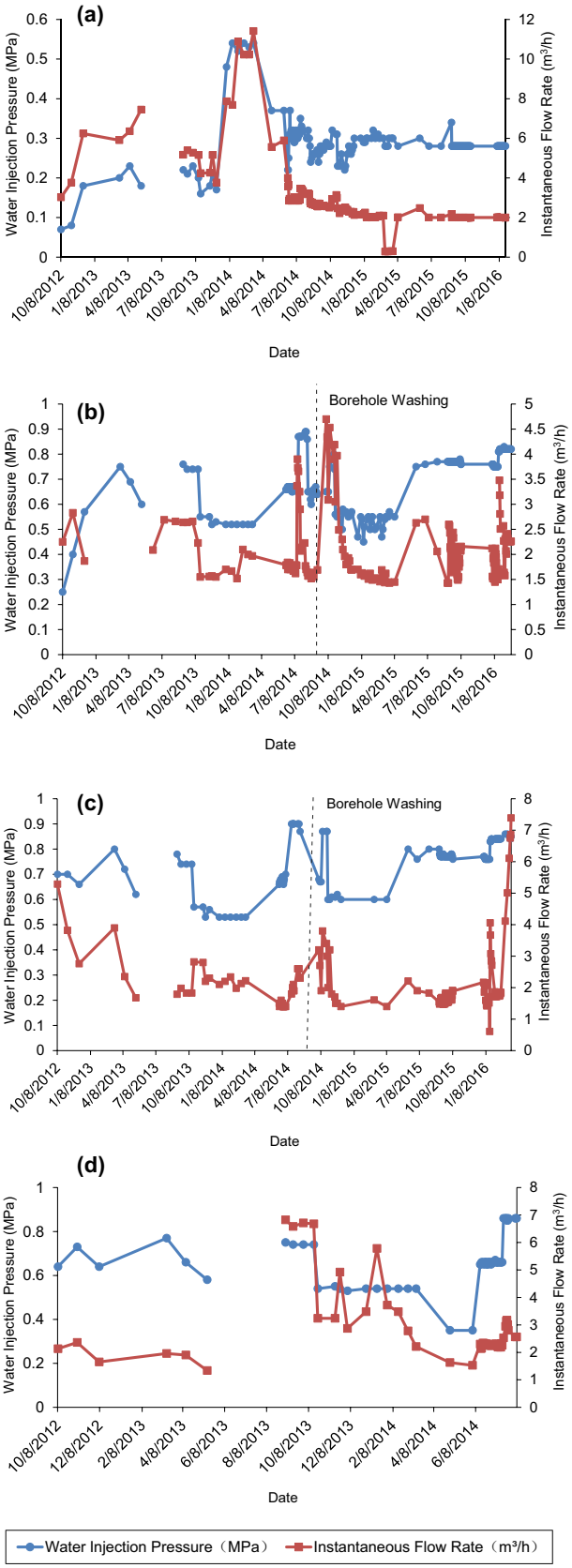

Fig. 2 Water injection pressures and flow rates in the injection boreholes **a** Z2, **b** Z4, **c** Z5, and **d** Z6 from October 2012 to March 2016

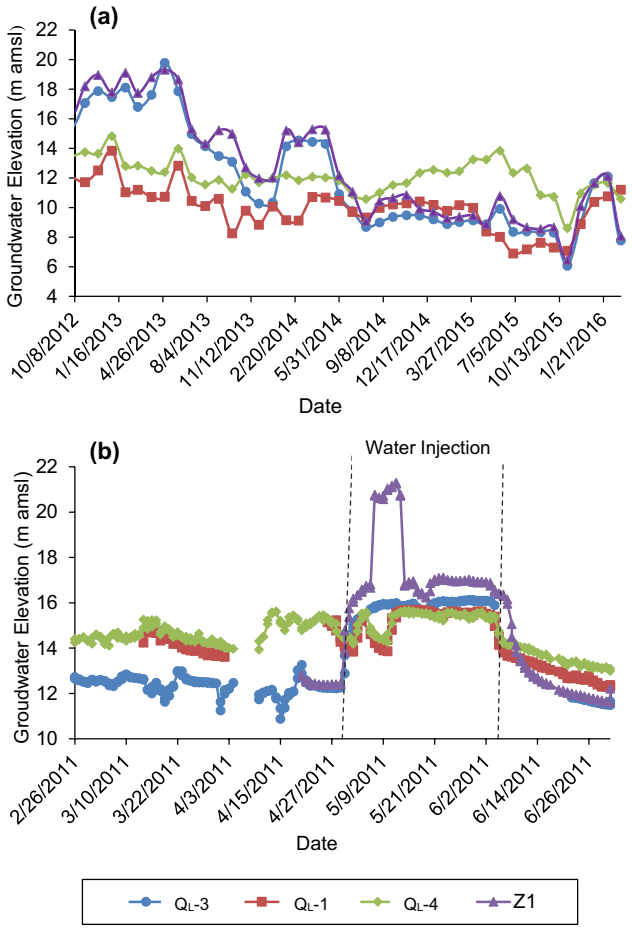

Fig. 3 Variation in groundwater elevation in the Q_L-3, Q_L-1, Q_L-4 and Z1 observation boreholes over time **a** during water injection from October 2012 to March 2016 and **b** during the combined injection test in the Z5 and Z6 boreholes

1 and 5 m^3/h; the injection pressure of the Z6 borehole was between 0.2 and 0.9 MPa, and the instantaneous flow rate was between 1 and 7 m^3/h. Results for the Z6 borehole after August 2014 are missing due to equipment malfunction. Although the instantaneous flow rate co-varied with the injection pressure on the whole, the injection flow rate was only about half of what it was during the combined injection test in the Z5 and Z6 boreholes. To increase the injection flow rate, the injection pressure was increased during the combined injection in the Z2, Z4, Z5, and Z6 boreholes. Nevertheless, the flow rate still decreased after a short increase. We consider that clogging at the base of water injection boreholes and migration of the fine particles around the permeable tube prevented a water flow increase.

Variation in Groundwater Elevation in the Observation Boreholes

Figure 3a shows the variation in groundwater elevation in the observation boreholes Q_L-3, Q_L-4, Q_L-1, and Z1 during water injection from October 2012 to March 2016, and Fig. 3b shows the variation in groundwater elevation in the four observation boreholes during water injection from April 29, 2011 to June 4, 2011. As shown in Fig. 3a, the groundwater elevation in the Q_L-3 borehole showed a general trend of "stable-downward-stable". Elevations in the Z1 borehole showed a general trend of "stable-downward", while elevations in the Q_L-1 and Q_L-4 boreholes showed a downward trend. From October 2012 to March 2016, the groundwater elevations in the Q_L-3, Z1, Q_L-1, and Q_L-4 boreholes dropped by 9.3, 10, 0.8, and 3 m, respectively. Groundwater elevations in the Q_L-3 and Z1 boreholes were relatively stable at first due to the early high flow rates in the Z2, Z4, and Z5 boreholes. After January 2016, groundwater elevations in the observation boreholes rose slightly, primarily due to the increase in injection rates in the Z4 and Z5 boreholes.

As shown in Fig. 3b, the groundwater elevation in the Q_L-3, Z1, Q_L-3, Q_L-4 boreholes increased during the combined injection test in the Z5 and Z6 boreholes. The groundwater elevations in the Q_L-3, Z1, Q_L-1, and Q_L-4 boreholes rose by 3.67, 4.16, 1.03, 1.77 m, respectively. The increase in the groundwater elevation in the Q_L-3 and Z1 boreholes was relatively larger than in the Q_L-1 and Q_L-4 boreholes because the depths of Q_L-3 and Z1 were closer to the injection depths. The monitoring depth of the Q_L-1 borehole was in the middle and lower units of the Quaternary alluvium and covered a large range, while the monitoring depth of the Q_L-4 borehole was in the middle unit of the Quaternary alluvium. However, the monitoring depths of the Q_L-3 and Z1 boreholes and the injection depths were in the lower unit (see Table 1).

Compared with the increase in groundwater elevation in the observation boreholes during the combined injection test (Fig. 3b), the smaller decrease in groundwater elevations from October 2012 to March 2016 (Fig. 3a) indicated that the injection flow rate was insufficient to maintain water level stability, and the effect of water injection weakened over time.

Strain Variation in Alluvial Strata

Figure 4a shows the strain variation in alluvial strata during the combined water injection (Z2, Z4, Z5, Z6) from October 2012 to March 2016, as measured by the FBG sensors. Figure 4b shows the changes in water level elevation in the Z1 borehole, as well as the strain variation measured by the FBG sensors in the corresponding alluvial strata during the combined injection test in the Z5 and Z6 boreholes from

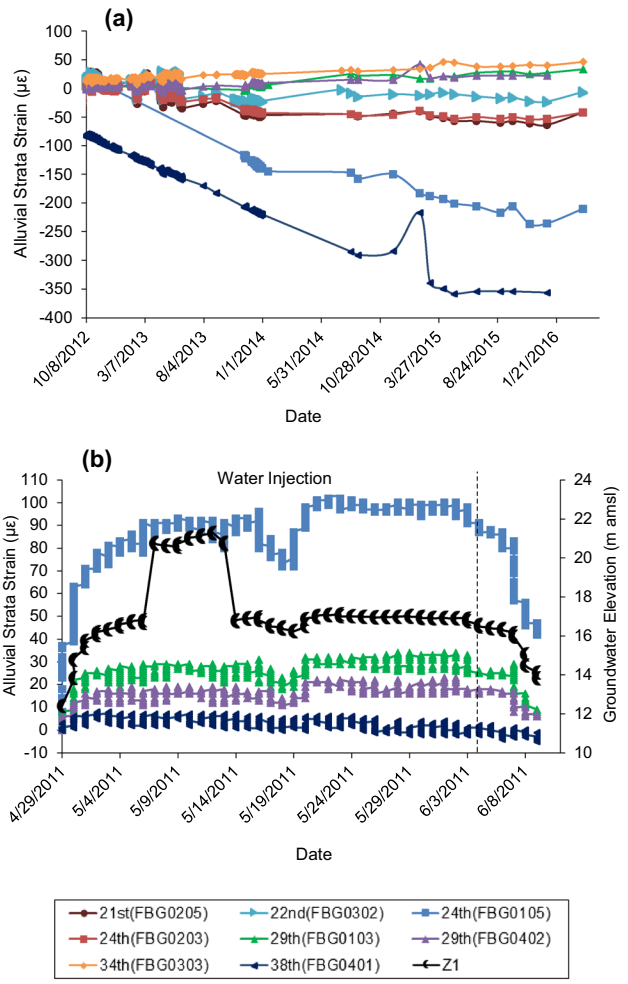

Fig. 4 **a** Strain variation in alluvial strata during the combined water injection (Z2, Z4, Z5, Z6) from October 2012 to March 2016, as measured in the FBG sensors and **b** variation in water level elevation in the Z1 borehole, as well as the strain variation measured in FBG sensors in corresponding alluvial strata during the combined injection test in the Z5 and Z6 boreholes from April 2011 to June 2011

April 2011 to June 2011; the end of the test is denoted by the dashed line.

Combined injection in the Z2, Z4, Z5, and Z6 boreholes

The strain in the 29th (FBG0402) and 34th layers remained positive and showed a slight increase, which indicated that tensile strain increased, and that the water injection played a positive role in terms of not creating compressive stress (Fig. 4a). However, strains in the 21st, 22nd, 24th (FBG0105 and FBG0203) and 38th layers became negative and decreased over time, indicating an increase in the compressive state of the alluvial layers. Strains in the 24th (FBG0105) and the 38th layers were increasingly negative (reaching as low as ≈ -250 and -350 με, respectively), also

indicating that compressive strain increased, the effect of water injection weakened, and the flow rate of water injection could not achieve strata stability. Mine dewatering has caused consolidation and compression of the strata, and the strain in layers increased continuously, indicating that the strata were becoming more compressed. In general, some compressive strain in the FBG monitoring points decreased during water injection from October 2012 to March 2016, while the compressive strain at most FBG monitoring points increased, indicating that the injection flow rate was insufficient and the positive effects of the injection weakened over time.

Combined Injection in Z5 and Z6 Boreholes

As shown in Fig. 4b, all strain values in the 24th (FBG0105) and 29th (FBG0103 and FBG0402) layers increased right after the water injection began, and the groundwater elevation in the Z1 borehole increased sharply at the same time, indicating that the water injection achieved good results initially in terms of not increasing compressive stress. Strain measurements in the 24th (FBG0105; after a decrease in mid-May) and 29th (FBG0103 and FBG0402) layers then kept increasing slightly through the end of the test, while measurements in the 38th layer decreased continuously and became negative in the end, which might be due to uneven water injection. Compared to elevations in the beginning of the test, the water level in the Z1 borehole rose by 4.2 m at the end of the test. Correspondingly, the strain values in the 24th (FBG0105) layer rebounded by 91 με; the strains in the 29th (FBG0103) layer rebounded by 26 με; and the strain in the 29th (FBG0402) layer rebounded by 18 με, indicating that the water injection created increasingly tensile, rather than compressive, stress conditions in the alluvial strata.

Obviously, there was a significant difference between water injection results for the two injection tests. Although mine dewatering caused consolidation of the alluvial strata, an adequate injection flow rate in the combined injection test in the Z5 and Z6 boreholes (Fig. 4a) resulted in a rising water level and the strata transitioning from a compressive state to a tensile state. The failure to keep the alluvial layers in a tensile state in the combined water injection in Z2, Z4, Z5, and Z6 boreholes (Fig. 4a) indicates that a higher injection flow rate appears to be needed to achieve water level stability during water injection.

Strain Variations in the Shaft Wall

Previous studies (Bi 1997) have shown that the shaft fractures were mainly caused by vertical compressive stress. Usually, the shaft wall fractures occurred near the interface between the alluvium and bedrock. Therefore, measuring the vertical strain variation in the shaft wall at the base of alluvium is very important.

Figure 5a–c show the variations in vertical strain over time in the ventilation shaft, the main shaft wall, and the auxiliary shaft wall, respectively, at the base of the alluvium from October 2012 to March 2016. Figure 5d shows the variation in groundwater elevation in the Q_L-3 borehole, as well as the strain variation in the corresponding ventilation shaft wall during the combined injection test in the Z5 and Z6 boreholes. Due to the lack of vertical strain data at the 167 m level of the main shaft wall, the strain variations in the main shaft wall were analyzed by taking measurements at the 159 m level. As shown in Fig. 5a, the vertical compressive strain at the 172 m level in the ventilation shaft wall increased, and the strain measured at the V2 borehole (northwest side) was close to − 800 με (warning value), which indicated that the risk of ventilation shaft failure was high. The vertical strain at the 159 m level in the main shaft wall fluctuated, and the compressive strain was slightly increased by the end of the measuring period (Fig. 5b), which indicated that the risk of the main shaft failing increased over time. However, compared with the ventilation shaft, the risk of main shaft failure was less. The strain variation in the auxiliary shaft wall (Fig. 5c) was similar to that in the ventilation shaft wall, and the vertical compressive strain at the 180 m level in the auxiliary shaft wall increased over time, indicating that the risk of shaft wall failure also increased over time. The strain measured at the V2 point (northeast side, Fig. 5c) was close to − 800 με (warning value), indicating an elevated risk of auxiliary shaft failure.

As shown in Fig. 5d, during the combined injection test in the Z5 and Z6 boreholes, groundwater elevation in the Q_L-3 borehole rose while the compressive strain at the 172 m level in the ventilation shaft wall decreased (became less negative). By the end of the combined injection test (see the dashed line in Fig. 5d), the water level in the Q_L-3 borehole rose by 3.7 m, and compressive strain at the V2 point rebounded by 56.5 με correspondingly, while the strain at the V3 point decreased by 55.9 με. These results show that when the water level rose by 1 m, the corresponding average strain at the V2 and V3 points rebounded by 15.4 and 15.2 με respectively, indicating that the water injection had achieved expected results and decreased the compressive strain in the shaft walls during the combined injection test in the Z5 and Z6 boreholes.

However, after the success of the injection test in the Z5 and Z6 boreholes, the vertical compressive strain measurements in the main shaft wall, the auxiliary shaft wall, and the ventilation shaft wall increased from October 2012 to March 2016 (Fig. 5a–c), showing that the effect of the water injection conducted in 2011 gradually weakened and water injection no longer reduce the compressive strain. Therefore,

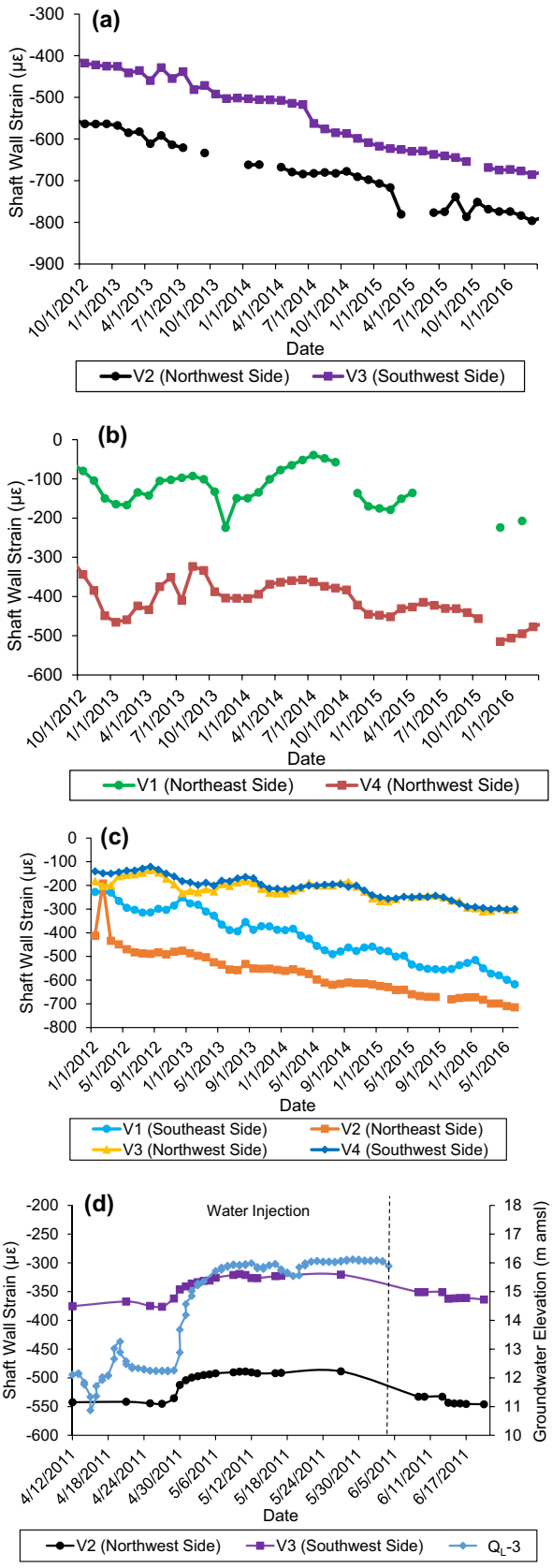

Fig. 5 **a** Vertical strain variation at the 172 m level in the ventilation shaft in recent years. **b** Vertical strain variation at the 159 m level in the main shaft in recent years. **c** Vertical strain variation at the 180 m level in the auxiliary shaft in recent years. **d** Variation in groundwater elevation in Q_L-3 borehole (right y-axis) and vertical strain variation (V2, V3) at the 172 m level (left y-axis) in the ventilation shaft during the combined injection test in the Z5 and Z6 boreholes

a higher injection flow rate was needed to reduce compressive stress.

Discussion

Variation in Water Injection Efficiency with Time

The water injection efficiency was defined as the quotient of the instantaneous flow rate and water injection pressure, in flow rate of water injection per hour per MPa:

$$\eta = \frac{Q}{P}, \tag{1}$$

where η is water injection efficiency (m^3/h/MPa); Q is instantaneous flow rate (m^3/h); and P is the water injection pressure (MPa). Figure 6 shows the changes in water injection efficiency with time in the injection boreholes from October 2012 to March 2016. The water injection efficiency in the Z2 injection borehole decreased significantly from 43.14 to 7.14 m^3/h/MPa. However, the water injection efficiency of the Z2 borehole was higher than that of the other injection boreholes because of less injection pressure in the Z2 borehole, rather than because of a higher injection flow rate. The injection efficiency of the Z4 and Z5 injection boreholes also decreased. However, in September 2014, there was a small increase in efficiency in boreholes Z4 and Z5, which was due to the borehole washing that reduced the water injection pressure and increased the injection flow rate. This indicated that borehole washing improved the injection efficiency in some cases. After September 2013, the injection efficiency decreased for the Z6 borehole, but due to the equipment replacement, measurements for the Z6 borehole were collected only before August 6, 2014. Although borehole washing improved the water injection efficiency and flow rate (see Supplemental Table 1, higher flow rate and lower pressure), the injection flow rate still decreased at the same pressure during a certain period of water injection, indicating that the effect of borehole washing was limited. The decrease in injection flow rate was mainly due to clogging of the permeable tube with fine particles. For the Z2, Z4, Z5, and Z6 boreholes, the efficiency of water injection decreased and the injection effectiveness generally weakened over time. However, the effect of the injection primarily depended on the water injection rate. Therefore, to improve the efficiency

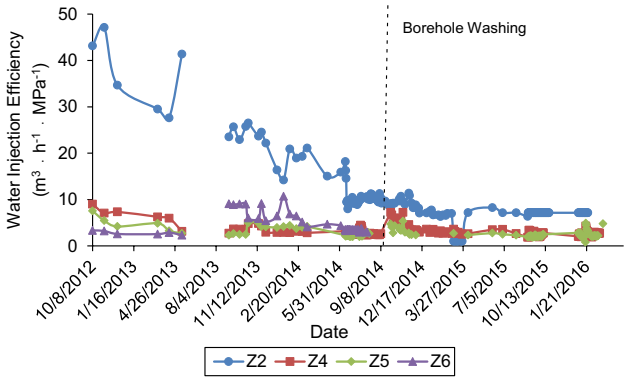

Fig. 6 Variations in water injection efficiency with time in the injection boreholes from October 2012 to March 2016

of water injection, it was also necessary to ensure that the injection rate met the requirements of water level stability.

Evaluation of the Effectiveness of Water Injection

Shaft failure results from the gradual drawdown of water level in the aquifer, which causes compression of alluvial strata and leads to fracture formation in the shaft wall. The decrease in strain in the shaft wall reflects the stress state there. A quantitative analysis of the effect of water injection was conducted using the strain variation over time in the shaft walls. A comparison of the slope of a linear regression of the strain data over time in the shaft wall before and during water injection could reflect the effectiveness of water injection. Figure 7a shows the strain in the ventilation shaft wall before water injection from June 20, 2008 to June 20, 2009 (June 20, 2008 is the zero point of the x-axis). For the injection period (October 8, 2012 to June 20, 2016), the linear regression started on October 8, 2012 and is the zero point of the x-axis (Fig. 7b). The measurements started a few months after the start date for water injection (Fig. 7b). The linear fitting relationship between vertical strain in the shaft walls and time is shown in Eq. (2):

$$\mu\varepsilon = kt + b, \tag{2}$$

where $\mu\varepsilon$ is microstrain; k is the slope of regression line; t is time in months after the start of water injection; and b is the y intercept of the regression line.

Table 4 shows the results for the regression parameters before any water injection was conducted (June 20, 2008–June 20, 2009) and during the ongoing combined water injection in the Z2, Z4, Z5, and Z6 boreholes (October 8, 2012–June 20, 2016) (k = slope; b = y intercept; R^2 = correlation coefficient). The R^2 in Table 4 is the correlation coefficient for the linear regression of strain and time.

The linear regression analysis shows that the correlation between vertical strain and time for the ventilation shaft

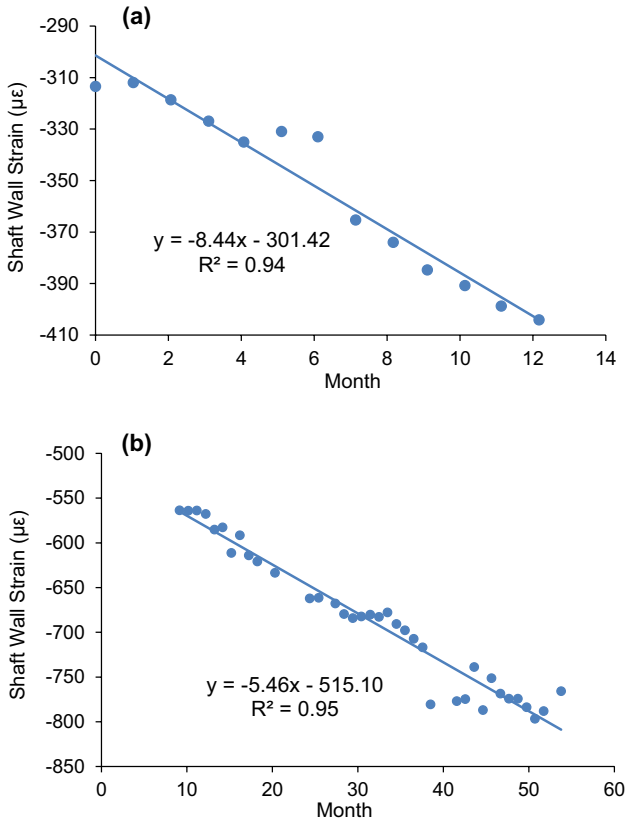

Fig. 7 Regression results for strain values over time in the ventilation shaft (at 172 m in V2 point) **a** before water injection that started on June 20, 2008 (zero point on x axis) and **b** during water injection that started on October 8, 2012 (zero point on x axis)

walls without and during the combined water injection in recent years were both strong: 0.94 and 0.95, respectively, for the V2 point at 172 m (see Fig. 7a, b). The correlation coefficients for vertical strain and time in the auxiliary shaft wall (at 180 m in V2 point) before and during water injection in recent years were 0.78 and 0.97, respectively. The correlation coefficients for vertical strain and time for the main shaft wall (at the 159 m level in V4 point) before and during water injection were 0.40 and 0.33, respectively, indicating poor correlation between the vertical strain and time. Nevertheless, it still could reflect the increase in compressive strain over time in the main shaft wall.

Overall, the slopes of linear regression in the main, ventilation, and auxiliary shaft wall before water injection were larger (more negative) than those during the combined water injection in the Z2, Z4, Z5, and Z6 boreholes, indicating that the strains in the main, ventilation and auxiliary shaft walls during injection were increasing less rapidly, suggesting that it was effective in reducing the risk of shaft failure. However, water injection did not change the increasing trend of compressive strain over time in the shaft walls.

Table 4 Regression results for vertical strain and time for the main, auxiliary, and ventilation shaft walls before any water injection was conducted (June 20, 2008–June 20, 2009) and during the ongoing combined water injection in the Z2, Z4, Z5, and Z6 boreholes (October 8, 2012–June 20, 2016) (k = slope; **b** = y intercept; R^2 = correlation coefficient)

Shaft name	Measuring point position	Before water injection (6/20/2008–6/20/2009)			During water injection in recent years (10/8/2012–6/20/2016)		
		k	b	R^2	k	b	R^2
Ventilation shaft	172 m level V2	− 8.44	− 301.42	0.94	− 5.46	− 515.10	0.95
Main shaft	159 m level V4	− 11.33	− 155.60	0.40	− 2.04	− 352.29	0.33
Auxiliary shaft	180 m level V2	− 17.55	− 99.84	0.78	− 5.12	− 440.47	0.97

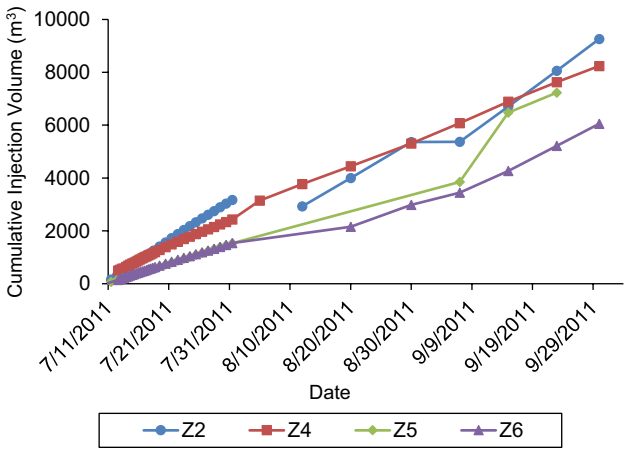

Fig. 8 Cumulative injection volumes for the Z2, Z4, Z5, and Z6 injection boreholes at an early stage (July 10, 2011 to September 23, 2011) of the water injection test

Determination of the Water Injection Rate

Figure 8 shows the cumulative injection volumes for the Z2, Z4, Z5, and Z6 boreholes at the beginning of the water injection test (July 10, 2011 to September 23, 2011). The cumulative flow volume for the Z2 borehole was 8060 m^3, and the average rate was 4.5 m^3/h; the cumulative flow volume for the Z4 borehole was 7623 m^3, and the average rate was 4.2 m^3/h; the cumulative flow volume for the Z5 borehole was 7230 m^3, and the average rate was 4.0 m^3/h; the cumulative flow volume for the Z6 borehole was 5217 m^3, and the average rate was 2.9 m^3/h. The cumulative flow volume for the four boreholes was 28,131 m^3, and the average rate was 15.6 m^3/h. The cumulative recovery (decrease) of compressive strain in the alluvial strata caused by water injection was ≈ 46.3 με. The average increased flow volume after injection was 1000 m^3, and the average recovery of strain in the alluvial strata was ≈ 1.6 με. Monitoring over a 22 month period before water injection from October 2007 to July 2009 (Dong 2010) showed that the monthly average strain in the alluvial strata was − 19.0 με, indicating that a monthly injection volume of ≈ 11,567 m^3 and an average injection rate of ≈ 4.0 m^3/h for each borehole could maintain the strata without subsidence. Combining the results from theoretical analysis and numerical simulation (Xu et al. 2014b) with the experience from the combined injection test in the Z5 and Z6 boreholes in this study, and considering unknown factors, such as instrumental error and the drawdown of the surrounding water level, the water should be injected at greater than 5.0 m^3/h per borehole to prevent shaft failure. This suggests that the total injection rate for the four boreholes should be more than 20 m^3/h.

The injection flow rate for the Z2, Z4, Z5, and Z6 boreholes early in the test (July 10, 2011 to September 23, 2011) was higher than later in the test (October 2012 to March 2016), and achieved the goal of maintaining the stability of the water level. From the latest flow volume data collected in June 2016, the weekly injection flow volumes for the Z2, Z4, Z5, and Z6 boreholes were approximately 160, 160, 190, and 700 m^3, respectively. According to the water injection flow calculated for March 2016, the monthly injection flow volume was approximately 5186 m^3, which was 44.8% of the monthly value required to maintain the strata without subsidence. Therefore, a higher injection flow rate was likely needed. Because of the clogging of the permeable tube with fine particles, measures such as oscillating the pressurized water injection or increasing the number of injection boreholes are suggested to increase the injection flow rate. If the effect of oscillating pressurized injection is poor, the injection flow rate could be increased only by increasing the number of injection boreholes.

Conclusions

We investigated the variation in groundwater elevation in four observation boreholes (Q_L-3, Q_L-4, Q_L-1, and Z1), measured the strains in the alluvial strata where water injection was conducted, and analyzed the stability of the ventilation, main, and auxiliary shafts in the Jining no. 3 coal mine

during water injection from October 2012 to March 2016. The following primary conclusions were reached:

1. During the water injection test in the Z2, Z4, Z5, and Z6 boreholes, groundwater elevations in the Q_L-3, Q_L-4, Q_L-1, and Z1 boreholes showed a decreasing trend over time on the whole, which was related to a decrease in groundwater elevation in the deepest part of the alluvial aquifer and water injection difficulties in the injection boreholes. The compressive strain in the alluvial layers increased over time, indicating that the water injection did not sufficiently reduce compressive strain in the strata and that they were still in a compressed state during this test.
2. More recently, the compressive strain at the base of the alluvium in the ventilation and auxiliary shafts increased over time, which indicated an increasing risk of ventilation and auxiliary shaft failure. The variability in strain at the base of the alluvium in the main shaft was smaller, indicating that the main shaft was relatively stable. The monitoring results for groundwater elevation and strain in the alluvial layers and the shaft walls showed that the effect of water injection weakened over time and a higher injection flow rate was needed.
3. More recently, the efficiency of water injection has generally decreased. The slopes of the linear regression between strain and time before and during water injection indicated that the water injection was effective in reducing the risk of shaft failure, but the compressive strain was still high later in the test. The combined injection test in the Z5 and Z6 boreholes was more effective than recent water injections in maintaining groundwater elevations and decreasing the risk of shaft failure.
4. Based on the experience from the combined injection test in the Z5 and Z6 boreholes, total and average injection rates for the four-borehole injection test needed to be ≈ 20 m^3/h and ≥ 5 m^3/h, respectively, to decrease the potential risk of shaft failure. To meet these requirements, measures such as borehole washing, oscillating pressurized water injection, or increasing the number of injection boreholes are suggested to prevent shaft failure.
5. Mining and dewatering activities in the Jining no. 3 mine have drained the alluvial aquifer. Most lost water volume in the aquifer seeped into the underground mine and was pumped to the ground surface through the mine drainage system. The risk of shaft failure will increase once injection is stopped. Indeed, due to the insufficient water injection rate and the weakening effect of water injection from October 2012 to March 2016, we are considering adding another injection borehole to increase the injection rate and thus achieve the goal of preventing shaft failure while mining is ongoing.

Acknowledgements We gratefully acknowledge the financial support provided by the National Basic Research Program of China (973 Program, 2013CB227903) and the National Natural Science Foundation of China (U1361209).

References

Baek J, Kim SW, Park HJ, Jung HS, Kim KD, Kim JW (2008) Analysis of ground subsidence in coal mining area using SAR interferometry. Geosci J 12(3):277–284

Bell FG, Bullock SET, Halbich TFJ, Lindsay P (2001) Environmental impacts associated with an abandoned mine in the Witbank coalfield, South Africa. Int J Coal Geol 45:195–216

Bi SW (1997) The research on the deformation mechanism and physical modeling 3D system of shaft failure in Xuhuai area. Syst Eng Theory Pract 17(3):42–48 **(in Chinese)**

Cui GX (1998) Mechanism and prevention of shaft fracture in special stratum. Min Construct Technol 19(4):28–32 **(in Chinese)**

Cui GX, Cheng XL (1991) Occasions of damaging shaft walls in Xuhuai district. Coal Sci Technol 8:46–50 **(in Chinese)**

Deng XL, Jiang CC, Xu YC, Li JH, Liang LM (2014) Analysis on effect of automatic water refilling method. Coal Eng 46(12):32–34 **(in Chinese)**

Dong L (2010) Study on monitoring experiment of water level and strain in huge unconsolidated soil layer. MS Thesis, Xi'an Univ of Sci and Technol, Xi'an City, China, pp 32–36 **(in Chinese)**

Gao J, Wang ZQ, Cheng JY, Zhang XJ (2009) Analysis of the additional stress induced by dewatering for the failure of shaft wall in the thick alluvium. Chin J Undergr Space Eng 5(5):873–877 **(in Chinese)**

Liu HY, Chen WZ, Wang ZM (2007) Theoretical analysis of shaft lining damage mechanism of Yanzhou mine. Chin J Rock Mech Eng 26(S1):2620–2626 **(in Chinese)**

Liu ZQ, Wang F, Guo Q (2011) Research progress on mine shaft liner breaking mechanism and prevention technologies in deep and thick overburden. Coal Sci Technol 39(4):6–10 **(in Chinese)**

Liu SQ, Jie YX, Xu YC (2017) Prevention of mine-shaft failure by aquifer replenishment. J Test Eval 45(3):889–903

Lou GD, Su LF (1991) Analysis of loading on shaft lining subjected to alluvium settlement due to water drainage. J Chin Coal Soc 16(4):54–61

Luo Y, Kimutis R, Yang K, Cheng JW (2010) Mitigation of longwall subsidence effects on an operating railroad. In: Proceedings of the 29th international conference on ground control in mining, Morgantown, WV, West Virginia University, pp 89–96 **(in Chinese)**

Meng ZQ, Ji HG, Peng F (2013) Additional stress of shaft linings in thick alluvium constructed by freezing process. China Coal Soc 38(2):204–208 **(in Chinese)**

Ni XH, Xu YC, Wang TF (2007) Mechanism and prevention of shaft fracture in thick alluvium. China Coal Industry Publishing House, Beijing **(in Chinese)**

Sato HP, Abe K, Ootaki O (2003) GPS-measured land subsidence in Ojiya City, Niigata Prefecture, Japan. Eng Geol 67:379–390

Sheorey PR, Loui JP, Singh KB, Singh SK (2000) Ground subsidence observations and a modified influence function method for complete subsidence prediction. Int J Rock Mech Min Sci 37:801–818

Soni AK, Singh KK, Prakash A, Singh KB, Chakraboraty AK (2007) Shallow cover over coal mining: a case study of subsidence at Kamptee colliery, Nagpur, India. Bull Eng Geol Environ 66:311–318

Tomaz A, Goran T (2003) Prediction of subsidence due to underground mining by artificial neural networks. Comput Geosci 29(5):627–637

Unver B, Yasitli NE (2006) Modelling of strata movement with a special reference to caving mechanism in thick seam coal mining. Int J Coal Geol 66:227–252

Wang WC (1996) Strength analysis of shaft based on surface subsidence caused by thick alluvium draining. J China Univ Min Technol 25(3):54–58 **(in Chinese)**

Wang CF, Chen ZS, Chen GF (2002) Comments on new technology of water injection to control mine shaft failure caused by ground subsidence. Coal Sci Technol 30(6):48–49 **(in Chinese)**

Xu YC, Li JH, Zhang Q, Wang X (2014a) Engineering parameters of water injection to control mine shaft damage at Jisan coal mine. J Liaoning Tech Univ (Nat Sci) 33(9):1153–1158 **(in Chinese)**

Xu YC, Li XD, Jie YX (2014b) Test on water-level stabilization and prevention of mine-shaft failure by means of groundwater injection. Geotech Test J 37(2):1–14 **(in Chinese)**

Yan SJ, Liu CL (1996) Status and prospect of urban land subsidence. Earth Sci Front 3(1–2):93–97 **(in Chinese)**

Yu Q (2013) Research on additional stress and ground settlement caused by dewatering in layered soils. Chin J Undergr Space Eng 9(1):166–172 **(in Chinese)**

Zhou GQ, Xu J (2006) Special shaft sinking and underground engineering in deep soil. Coal Industry Press, Beijing **(in Chinese)**